

Correlations between the Hall coefficient and the superconducting transport properties of oxygen-deficient $\text{YBa}_2\text{Cu}_3\text{O}_{7-\delta}$ epitaxial thin films

E. C. Jones

Department of Physics, University of Tennessee, Knoxville, Tennessee 37996-1200

D. K. Christen

Solid State Division, Oak Ridge National Laboratory, Oak Ridge, Tennessee 37831-6061

J. R. Thompson

*Department of Physics, University of Tennessee, Knoxville, Tennessee 37996-1200
and Solid State Division, Oak Ridge National Laboratory, Oak Ridge, Tennessee 37831-6061*

R. Feenstra

Solid State Division, Oak Ridge National Laboratory, Oak Ridge, Tennessee 37831-6061

S. Zhu

Department of Physics, University of Tennessee, Knoxville, Tennessee 37996-1200

D. H. Lowndes

Solid State Division, Oak Ridge National Laboratory, Oak Ridge, Tennessee 37831-6061

Julia M. Phillips and M. P. Siegal*

AT&T Bell Laboratories, 600 Mountain Avenue, Murray Hill, New Jersey 07974

J. D. Budai

Solid State Division, Oak Ridge National Laboratory, Oak Ridge, Tennessee 37831-6061

(Received 20 October 1992; revised manuscript received 18 December 1992)

Strong correlations between the Hall coefficient R_H , the transition temperature T_c , and the critical current density J_c were established in a series of epitaxial $\text{YBa}_2\text{Cu}_3\text{O}_{7-\delta}$ thin films as a function of oxygen deficiency δ . Steady increases in R_H with δ suggest that deoxygenation reduces the density of states which, according to BCS theory, should lead to corresponding decreases in T_c . In contrast, two well-known plateaus occurring at 90 K and 60 K were observed in T_c vs δ . Others have ascribed these plateaus to either electronic phenomena or phase separations. We find that in the 90-K plateau, the critical current density $J_c(\delta, H=0)$ decreases with δ and extrapolates toward zero at the edge of the plateau, while the relative-field dependence of $J_c(\delta, H)$ and the flux-creep pinning energies are independent of δ . These observations suggest that the phase-separation scenario occurs on the 90-K plateau. However, electronic origins cannot be ruled out at present due to difficulties in determining the equilibrium superconducting properties of oxygen-deficient $\text{YBa}_2\text{Cu}_3\text{O}_{7-\delta}$ films.

I. INTRODUCTION

Early work on oxygen-deficient $\text{YBa}_2\text{Cu}_3\text{O}_{7-\delta}$ led to the discovery of two plateaus in $T_c(\delta)$ that are now well known.¹ More recently, it was found that these plateaus are absent in samples prepared by rapid quenching from high temperatures.^{2,3} Although the origin of these features has proved difficult to elucidate, several elaborate electronic models have been proposed that rely either on a two-gap mechanism,⁴ or on charge transfer from the Cu-O chains to the Cu-O₂ planes.^{5,6} However, magnetic hysteresis studies clearly show anomalous critical current density $J_c(H)$ enhancements in applied fields $H > 0$ which have been attributed to defect clustering in oxygen-deficient bulk samples.^{7,8} Electron-diffraction

studies^{9,10} and one neutron-diffraction study¹¹ have indicated that a discrete series of ordered superstructures, having small differences in oxygen deficiency, are simultaneously present, but only on the T_c plateaus. If the size of such domains exceeds that of the coherence length ξ (~ 20 Å), then these domains should exist with distinct T_c values. A fundamental understanding of the plateaus requires knowledge of the nature of these domains. If regions of distinct T_c 's exist, experiments inducing finite electric fields would tend to generate normal currents, thereby averaging over the phase distribution. On the other hand, transport studies at the limit of relatively small electric fields ($1 \mu\text{V}/\text{cm}$) would greatly emphasize only the highest critical current-density J_c phases, providing insight into the validity of the phase-separation

scenario. In this work, we examine correlations between the Hall coefficient R_H , T_c , and J_c in a series of epitaxial thin films that were rendered oxygen deficient by thermal processing under controlled conditions. The results presented here are based on two samples representative of the highest quality thin films.

II. EXPERIMENTAL ASPECTS

The epitaxial thin films were grown either by the BaF_2 process¹² or by pulsed laser ablation onto LaAlO_3 substrates.¹³ For transport measurements, the c -axis perpendicular films were photolithographically patterned with a 3-mm long by 50- μm wide bridge containing two opposing 20- μm wide Hall terminals. Six gold dots were then sputtered onto contact areas to allow simultaneous measurements of the resistive and Hall signals using standard dc techniques. Currents were systematically reversed to eliminate thermal emf's. Contact resistances were less than 0.1 m Ω after the first full oxygenation anneal at 550°C in 1 atm O_2 . This allowed easy, solder-free mounting and demounting with the use of Au-In-Au pressure pads and spring loaded "pogo" contacts. To control the oxygen deficiency δ , we conducted sequential isobaric anneals¹⁴ at 550°C under reduced partial pressure of O_2 . Thus, small changes in T_c , J_c , and R_H as a function of δ could be obtained in a given sample of fixed bridge geometry, thereby eliminating the relative errors due to cross-sectional differences. The effects of oxygen de-

pletion were reversible, as demonstrated by a final anneal at 1 atm O_2 that reestablished the starting properties of the films even after 11 sequential anneals. To eliminate offset voltages due to the physical Hall terminal mismatches and to the transverse-even field¹⁵ R_{TE} , the Hall coefficient in the limit of low fields was defined by the difference of the Hall resistivities taken in opposing fields,

$$R_H = \frac{\rho_{yx}(H) - \rho_{yx}(-H)}{2H}. \quad (1)$$

Magnetic fields of 8 T were applied parallel to the c axis, and were verified to be in the low-field regime,¹⁵ since linear R_H vs B behavior was observed up to 8 T while in the normal state for all oxygen deficiencies.

From systematic x-ray-diffraction studies of four films, we obtained the following correlation between the relative change in the c -axis lattice parameter c and the normal-state electrical conductivity σ , for oxygen contents in the regime of the 90-K plateau:

$$\frac{\Delta c}{c_0} = (4.8 \pm 0.5) \times 10^{-3} \frac{\Delta \sigma}{\sigma_0}, \quad (2)$$

where c_0 and σ_0 represent the fully oxygenated state.¹⁶ In bulk $\text{YBa}_2\text{Cu}_3\text{O}_{7-\delta}$, the c -lattice expansion has been correlated with the oxygen deficiency δ in the orthorhombic state according to the average results of Cava *et al.* and Jorgensen *et al.*:^{17,18}

TABLE I. Experimental data used in the determination of δ 's depicted in the figures for the two representative samples. The calculations of δ are described in the text and are rounded to the nearest 0.05. The letters q and a denote quenched from 200°C and aged at room temperature for 4 days, respectively.

Figure(s)	Est. $7 - \delta$	J_c (1.2 K) (A/cm ²)	Growth process	Anneal $\log_{10}(P_{\text{O}_2})$	$ \Delta\sigma/\sigma_0 $ (100 K)	T_c (1%) (K)	
3(a)	7.0	1.47×10^7	BaF ₂	1 atm	0	89.4	
3(a)	6.9	7.40×10^6		-0.60	0.201	90.4	
3(a)	6.8	3.16×10^6		-0.97	0.430	89.6	
3(a)	6.7	6.50×10^5		-1.56	0.650	74.5	
3(a), 4	6.6	1.58×10^5		-2.14	0.678	60.5	
3(a)	6.5	1.00×10^5		-2.50	0.702	54.0	
3(a)	6.4	$\approx 1 \times 10^4$		-3.00	0.903 a	29.0 a	
1, 3(b), 6(a)	7.00	2.50×10^7		Laser ablation	1 atm	0	88.3
3(b), 6(a)	6.95	Not obtained			-0.60	0.110	88.9
1, 3(b), 6(a)	6.90				-1.00	0.210	89.4
1, 3(b), 6(a)	6.85		-1.48		0.355	88.8	
1, 3(b), 4, 6(a)	6.80		-1.78		0.460	87.0	
1, 3(b), 4	6.70		-2.09		0.645	76.0	
1, 4	6.50		-2.53		0.719	56.2	
1	6.45		-3.05		0.835 q	38.0 q	
					0.824 a	42.0 a	
1, 3(b)	6.40		-3.25		0.906 q	12.0 q	
				0.897 a	20.0 a		
1	6.35		-3.55	0.967 q	Insulating		
				0.963 a			

$$\frac{1}{c_0} \frac{\Delta c}{\Delta \delta} = +10.7 \times 10^{-3}. \quad (3)$$

Combining Eqs. (2) and (3) leads to the result

$$\delta \approx 0.45 \left| \frac{\Delta \sigma}{\sigma_0} \right|. \quad (4)$$

Values of δ obtained from Eq. (4) must be regarded as provisional, since extrinsic factors such as substrate-induced strains may alter both the magnitude of the c -lattice parameter, as well as its response to δ . The values are quoted to provide a familiar and relative labeling of composition, but *none* of the following analyses depend quantitatively on the precision of the values. With this proviso, we tabulate in Table I experimental information associated with the determination of the δ values for the two representative samples used in the figures. Since Eq. (4) generates a maximum value of only $\delta = 0.45$, e.g., $|\Delta \sigma / \sigma_0| \rightarrow 1$, this equation was utilized for the estimates of δ only in the range in which the x-ray data were obtained, i.e., $\delta \leq 0.3$. For larger oxygen deficiencies, δ was based entirely on the comparisons of T_c to those published by Veal and Paulikas and Jorgensen *et al.*^{6,18}

III. OVERVIEW OF EXPERIMENTAL RESULTS

Before discussing in detail each of the experimental results, we present here a brief overview of the principal findings. The electrical transport properties of $\text{YBa}_2\text{Cu}_3\text{O}_{7-\delta}$ vary systematically with increasing oxygen deficiency δ . Both the resistivity $\rho(\delta)$ and the Hall coefficient $R_H(\delta)$ increased with δ at similar rates, and consequently the Hall angle, given by $\tan(\theta_H) \equiv R_H B / \rho$, changes only slightly (Fig. 1). In *all* films, the critical current densities $J_c(\delta, H=0)$ measured in self-field extrapolated towards zero for compositions near the edge of the 90-K plateau (Fig. 2), while the temperature and field dependencies of $J_c / J_c(H=0)$ (Fig. 3) remained fixed for $\delta < 0.15$, both of which are suggestive of geometrical effects. For larger oxygen deficiencies ($\delta > 0.3$), the field dependencies of $J_c(\delta, H)$ were similar to those observed in polycrystalline $\text{YBa}_2\text{Cu}_3\text{O}_7$ and the flux-flow Hall transitions exhibited systematic “noise” (Fig. 4), indicative of granularlike behavior. Pinning energies determined both from the field dependence of $J_c / J_c(H=0)$ and from in-field resistive transitions (Figs. 5 and 6) show plateaulike behavior near full oxygenation even though J_c decreases rapidly in this region. On the 90-K plateau, most films showed no broadening in the resistive transitions; however, *all* films showed some broadening in the transitions between the 90-K and 60-K plateaus. Films postannealed at low PO_2 usually showed “peaked” T_c behaviors with δ , unlike the high PO_2 postannealed films which typically show “flat” 90-K plateaus.¹⁹ However, the Hall coefficients (Fig. 7) were found not to rely on the processing conditions, suggesting that differences in the measurable carrier densities are not responsible for these different $T_c(\delta)$ patterns.

IV. DISCUSSION OF RESULTS

A. Effect of oxygen deficiency δ on the resistivity and Hall coefficient

The removal of oxygen from $\text{YBa}_2\text{Cu}_3\text{O}_{7-\delta}$ leads to a progressive increase in the resistivity [Fig. 1(a)] as well as a decrease in Hall number [Fig. 1(b)]. These observations suggest steady decreases in the density of states which, according to simple BCS theory, should lead to steady decreases in T_c . In actuality, two plateaus are observed in T_c vs δ which could be reconciled either by phase separation^{9,11} or by some complex electronic mechanism.^{4,5}

Interestingly, the insets of these figures show the effects of room-temperature annealing which may be ascribed to the formation of oxygen-ordered “Ortho-II” phase at fixed $\delta \geq 0.4$.⁶ These room-temperature ordering effects were studied at three estimated oxygen contents of 6.35, 6.40, and 6.45. For investigation at each of these fixed oxygen contents, the sample was quenched from 200°C, rapidly mounted, and cooled below 250 K in about 30 min. No ordering effects were ever observed during measurements at $T < 250$ K, and the final results are depicted by the dashed curves in Figs. 1(a) and 1(b). After completion of each data acquisition sequence, the sample was warmed to room temperature, and allowed to age until the resistivity reached a minimum saturation—approximately four days at each oxygen content. These results are depicted by solid curves in the same figures. In addition to an observed reduction in resistivity [time dependence given by Eq. (5)], this ordering-related annealing always led to an increase of the observed Hall number and transition temperature (see Table I), which could be interpreted as an indication of additional charge carriers being transferred to the Cu-O_2 planes as suggested by the electronic model first proposed by Veal and Paulikas.⁶ In a similar fashion to that of Veal *et al.*²⁰ our aging data taken near $7-\delta \approx 6.45$ were found to be well described by

$$R(t) = R(t = \infty) - [R(t = \infty) - R(t = 0)] \exp(-\sqrt{t/\tau}), \quad (5)$$

where $R(t)$ is the resistance at time t after the quench and τ is a relaxation time given by $\tau = A \exp(\Delta E / k_B T)$. From this analysis, the prefactor A and activation energy ΔE were found to be 1.4×10^{-12} s and 0.95 ± 0.02 eV, respectively, in good agreement with Veal’s aging studies on bulk $\text{YBa}_2\text{Cu}_3\text{O}_{\approx 6.5}$ crystals. This suggests that substrate-induced strains in thin films have little or no effect on the oxygen-ordering processes in the Ortho-II phase. More important, these observations do not rule out a phase-separation scenario, since a parallel configuration of two dissimilar conductors (denoted by indices 1 and 2) will yield an observed Hall coefficient R_H given by

$$R_H = \frac{R_2 R_{H1} + R_1 R_{H2}}{R_1 + R_2}, \quad (6)$$

where R_{Hi} and R_i refer to the Hall coefficient and the resistance contributed by the i th conductor, respectively.

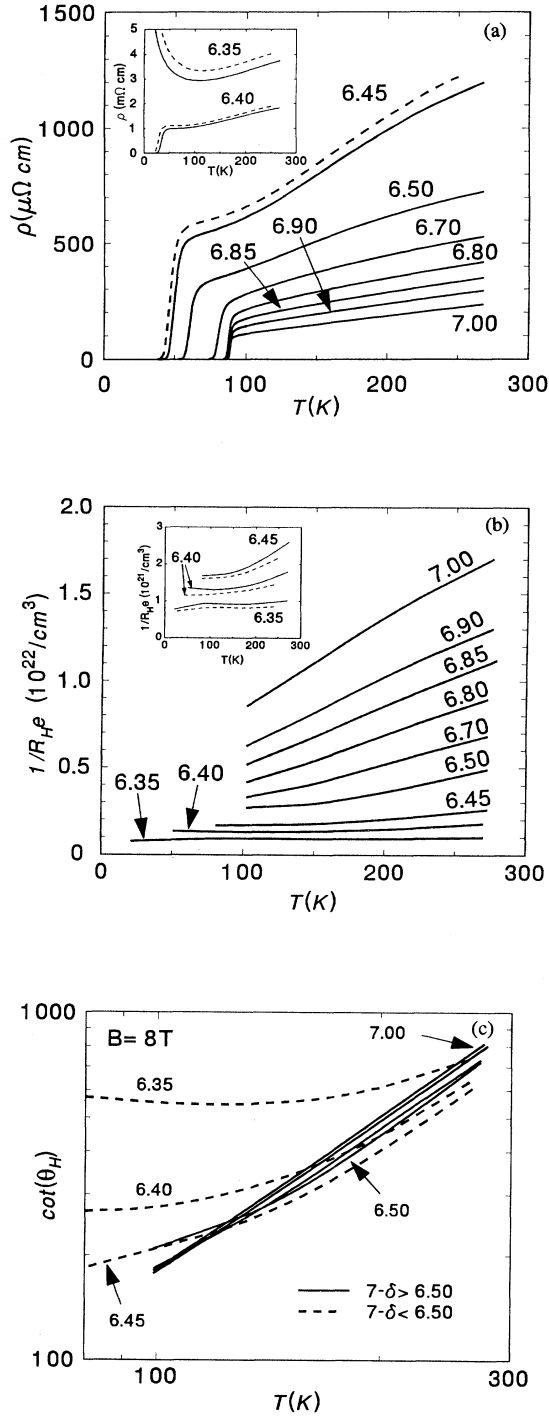


FIG. 1. Resistivity (a), inverse Hall coefficient (b), and inverse Hall angle (c) for a laser-ablated film of $\text{YBa}_2\text{Cu}_3\text{O}_{7-\delta}$ as a function of temperature and oxygen deficiency δ . Insets show the apparent changes in the Ortho-II phase with room-temperature annealing. The dashed curves in parts (a) and (b) represent the behavior immediately after quenching from 200°C , whereas the corresponding solid curves represent the behavior after aging for 4 days. The inverse Hall angle is shown on a log-log plot to depict the relative insensitivity of the T^2 behavior to oxygen deficiency.

It is clear from this equation that the phase contributing the least electrical resistance would average more heavily in the apparent Hall coefficient. Moreover, if phase separation leads to a larger proportion of the “better” phase, i.e., lesser resistivity and higher oxygen content, the apparent value of R_H would decrease with room-temperature annealing. This would occur because the aging process would create a larger proportion (i.e., less resistance) of the phase having the smaller value of R_H [see Fig. 1(b)]. Therefore, the normal-state resistivity and normal-state Hall coefficient results alone cannot determine whether or not phase separation occurs in oxygen-deficient $\text{YBa}_2\text{Cu}_3\text{O}_{7-\delta}$.

Another feature of Fig. 1(a), which is observed in all samples, is a slight broadening of the resistive transitions off the 90-K plateau. It is unlikely that this broadening results from the formation during cooldown of layers with differing oxygen contents, since no 90-K onsets are observed for compositions off the 90-K plateau [see Fig. 1(a)]. Rather, this broadening off the 90-K plateau is most likely due to a T_c distribution, with a series connection of domains with different T_c 's.

A potentially important finding is the relative constancy of the Hall angle $\tan(\theta_H) = E_y/E_x = R_H B/\rho$ for oxygen deficiencies δ when $\delta \leq 0.5$ [Fig. 1(c)]. In a multiband system, the Hall angle can be derived from simple expressions for a multiband system²¹

$$\tan(\theta_H) = \frac{E_y}{E_x} = \frac{B_z}{\sigma} \sum_i R_{Hi} \sigma_i^2. \quad (7)$$

Assuming each (parabolic) band can be described by the expressions $R_{Hi} = -1/n_i e$ and conductivity $\sigma_i = n_i e^2 \tau_i / m_i$, this becomes

$$\tan(\theta_H) = -\frac{1}{\sigma} \sum_i \omega_i \tau_i \sigma_i. \quad (8)$$

Here $\omega_i = eB/m_i$ and τ_i are the cyclotron frequencies and relaxation times for the i th band, respectively. Moreover, the band-structure calculations predict four bands crossing the Fermi level in $\text{YBa}_2\text{Cu}_3\text{O}_7$, and each of these bands is expected to have different effective masses.²² Therefore, it is plausible that, upon oxygen depletion the individual conductivities would change at different rates. Under these circumstances, Eq. (8) suggests that significant deviations should occur in the observed magnitude and temperature dependence of the Hall angle with changing oxygen deficiency. On the contrary, the Hall angle changes only slightly over most of the oxygen content range [Fig. 1(c)] and this suggests that one band dominates the normal-state properties with fields $H \parallel c$.

B. Temperature dependence of the Hall coefficient

To understand the temperature dependence of the Hall coefficient, we use the proposal that $\text{YBa}_2\text{Cu}_3\text{O}_7$ behaves as a two-dimensional Luttinger liquid.²³ Use of this single-band theory is justified by and consistent with the arguments just presented. In this formalism, the observed Hall angle $\tan(\theta_H)$ depends on a “transverse” relaxation rate τ as

$$\cot(\theta_H) = (\omega_c \tau)^{-1} = AT^2 + (\omega_c \tau_{\text{imp}})^{-1}.$$

Here ω_c is the field-dependent cyclotron frequency and $1/\tau_{\text{imp}}$ is the scattering rate due to impurities. In a Luttinger liquid, separation occurs between the charge and spin quasiparticles. Furthermore, application of a magnetic field leads to the rotation of k space allowing the transverse relaxation rate to include only the effects of the spin-spin interactions. Being fermions, these interactions should lead to the well-established T^2 scattering process in $\cot(\theta_H)$, whereas the impurity scattering term only includes the effects of magnetic scattering centers. Referring to the log-log plot [Fig. 1(c)], the inverse Hall angle indeed varies as T^2 over a wide range of oxygen deficiencies ($\delta \leq 0.55$) in $\text{YBa}_2\text{Cu}_3\text{O}_{7-\delta}$. On the other hand, a transport relaxation rate τ_{tr} is measured in the resistivity and is proportional to the decay rate of the accelerated electrons into elementary excitations (holons and spinons), such that

$$\rho \propto \frac{m}{ne^2} \left[\frac{1}{\tau_{\text{tr}}} + \frac{1}{\tau_{\text{imp}}} \right], \quad (9)$$

where²³ $\tau_{\text{tr}}^{-1} \propto T$. In relatively clean materials, the impurity scattering rate $1/\tau_{\text{imp}}$ may be neglected. Combining these results, one has $1/(R_H e) \propto \cot(\theta_H)/\rho \propto nT$, where n is the density of charge carriers and e is the electron charge. Thus, within the Luttinger liquid approach, the average slopes of the inverse Hall coefficient curves, which vary almost linearly with temperature [Fig. 1(b)], serve as a relevant electronic parameter for displaying our data. In Fig. 2 are plotted the transition temperatures $T_c(R=0)$ and $T_c(\text{mid})$ as well as the critical current densities in self-field $J_c(\delta, H=0)$, as a function of

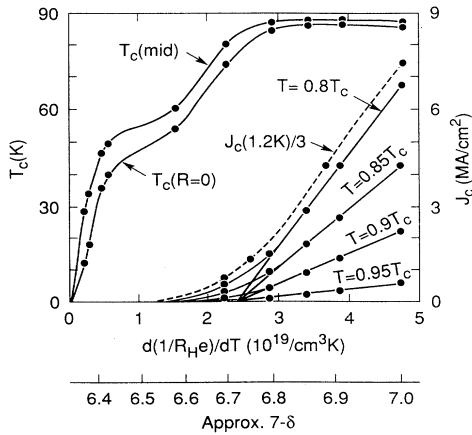


FIG. 2. Transition temperature T_c , and critical current density J_c evaluated at fixed reduced temperatures, as a function of either the oxygen deficiency δ or the “apparent carrier density” from the Luttinger liquid theory described in the text. Notice that J_c extrapolates toward zero at the edge of the 90-K plateau, suggestive of phase separation. The solid (dashed) curves were obtained from a laser-ablated (BaF_2 processed) film. Extrapolations do not occur at exactly the same point due to uncertainties in the film thickness.

$d(1/R_H e)/dT$. Note that a simpler plot of superconducting properties, e.g., T_c and J_c , as a function of $1/(R_H e)$ would give qualitatively similar results [see Fig. 1(b)]; however, the function $1/(R_H e)$ must be chosen at an arbitrarily fixed temperature when displaying data in this fashion. Overall, most superconducting properties improve with increasing $d(1/R_H e)/dT$.

Although this behavior is consistent with the Luttinger liquid model, alternate explanations for the temperature dependence of $1/(R_H e)$ may be found in a sharp peak in the electronic density of states (DOS) lying near the Fermi surface.^{24,25} The existence of such a van Hove singularity (vHs) is suggested in the band structure;^{22,26} however, band-structure calculations place the DOS peak ~ 0.1 eV below the Fermi energy. According to Pickett,²⁷ this DOS peak is associated with the chain layer-derived bands, which are more difficult to determine accurately than the plane-related bands. Interestingly, these same chain-related bands in the 60-K phase, $\text{YBa}_2\text{Cu}_3\text{O}_{6.5}$, lie farther below the Fermi surface, according to Yu.²⁸ In this picture, the systematic decrease in the temperature dependence of R_H with δ merely reflects a steady displacement of the peaked DOS (vHs) from the Fermi energy. To be plausible, however, this scenario requires that the peak is actually nearer to the Fermi surface than calculated.

Yet another possible explanation comes from Bloch-Boltzmann theory. These calculations, however, are complicated and the Fermi-Dirac distribution $-\partial f/\partial \epsilon$ must often be approximated by $\delta(\epsilon - \epsilon_F)$. Moreover, the standard approximation of isotropic scattering leads²⁹ to a temperature-independent R_H . Interestingly, Ong³⁰ has shown that, in the framework of this conventional theory, a temperature-dependent R_H can result from a changing anisotropy of the ab -plane “scattering path length” vector $l(\mathbf{k}) = \mathbf{v}_k \tau_k$ with temperature T . Nevertheless, these latter mechanisms may prove difficult in explaining the universal quadratic temperature dependence of the inverse Hall angle, $\cot(\theta_H) = AT^2 + B$ [Fig. 1(c)]. Finally, this quadratic temperature dependence is also reported well above the Debye temperature³¹ which tends to support a nonphononic scattering mechanism.

C. Effect of oxygen deficiency δ on the critical current density

We now consider the transport critical current density J_c , measured in self-field. Examination of Table I and Fig. 2 shows that J_c extrapolates toward zero at an oxygen deficiency near the edge of the 90-K plateau. This feature was observed in *all* films, and somewhat similar behavior was reported earlier by Ossandon *et al.*³² in magnetic measurements of current density in bulk, aligned $\text{YBa}_2\text{Cu}_3\text{O}_{7-\delta}$. For $\delta \leq 0.15$, J_c varies linearly with δ . In this regime, the functional dependencies of J_c on temperature and field [Fig. 3] are constant, which suggests a geometrical decrease in the amount of 90-K phase. In this view, $J_c(\delta)$ deviates from its linear decrease with δ for compositions $\delta \geq 0.15$ because other, lower J_c phases then conduct appreciable portions of the supercurrent. This tapering occurs near the same oxygen

content at which the field dependencies of J_c begin to degrade. This degradation implies reductions in the pinning energy, as discussed below.

D. Determination of the pinning energy

Several methods provide means of determining the pinning energy. These include analyses of I - V curves, resis-

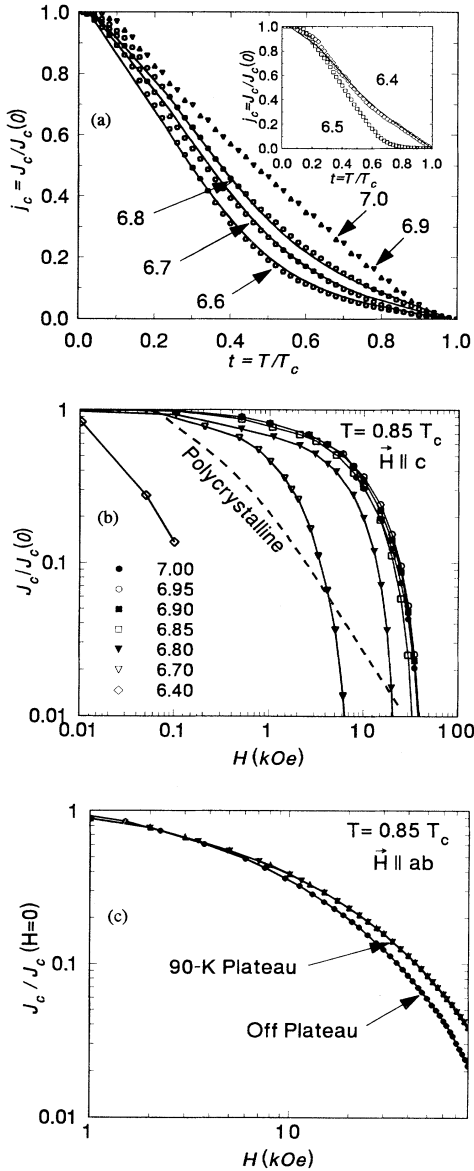


FIG. 3. Reduced critical current densities as a function of temperature (a), applied field for $H \parallel c$ (b), and applied field for $H \parallel ab$ (c) for various oxygen contents. No apparent changes in pinning energy occur while on the 90-K plateau even though $J_c(0)$ decreases rapidly (see Table I). Interestingly, many of the curves in (a) behave as SNS proximity tunneling (Ref. 49) (solid curves) off the 90-K plateau. The dashed curve is a representative polycrystalline sample (Ref. 38) which indicates the granular-like behavior when $\delta > 0.2$.

tive transitions $\rho(T, H)$, or dependencies of critical currents $J_c(T, H)$ on field. Recently, self-consistent values for the pinning energies were obtained in fully oxygenated $\text{YBa}_2\text{Cu}_3\text{O}_7$ epitaxial films determined from the I - V curves and from in-field resistive transitions.³³ However, if phase separation occurs in oxygen-deficient $\text{YBa}_2\text{Cu}_3\text{O}_{7-\delta}$, the I - V curves would clearly be difficult to interpret, since the actual current path dimensions, which are required to calculate the flux-creep resistivities, would be unknown. Similarly, Arrhenius plots of the resistive transitions would be expected to broaden (theoretically shown by others^{34,35}) as a result of inhomogeneities. For example, the apparent T_c distributions observed in the Hall transitions in Fig. 4 would probably lead to errors in the derived pinning energies. Note also that, on the 90-K plateau, J_c decreases by roughly an order of magnitude while the conductivity decreases by a factor of only 1.8. As a result, the derived pinning energies obtained under relatively high electric fields, i.e., resistive transitions, may be in error due to induced normal currents in the lower T_c phases which are forced normal by the applied magnetic fields.

To develop this more rigorously, we consider the standard expression for the creep resistivity:³⁶

$$\rho = \frac{E_0}{J_{c0}} \frac{U_0(T, B)}{kT} \exp \left[-\frac{U_0(T, B)}{kT} \right], \quad (10)$$

which is valid in the limit of small current and thus is applicable to the resistive transition measurements. Here J_{c0} is the critical current density in the absence of flux creep, E_0 is proportional to the elementary "attempt" frequency, and U_0 is the activation energy for flux creep. Due to the weak, logarithmic sensitivity of the analysis, the prefactor is generally approximated to be constant. It follows that the slopes of the Arrhenius plots of $\ln \rho$ vs $1/T$ are equal to $-U_0(T, B)/k$. The situation becomes more complex in the phase-separation scenario. Using the resistor combination equations,

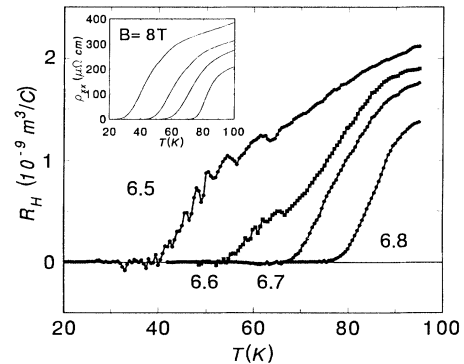


FIG. 4. Flux-flow Hall coefficients taken at 8 T for various oxygen contents. All Hall transitions with $\delta \geq 0.3$ show reproducible "onsets" indicative of a distribution of T_c 's. However, these onsets were never observed on the 90-K plateau nor in any resistive transition as shown in the inset.

$$\rho^{\pm 1} = \sum_i^n f_i \rho_i^{\pm 1}, \quad (11)$$

where f_i denotes the volume fraction of the i th phase, and + or - specifies series or parallel combinations, respectively, the Arrhenius equation becomes

$$\ln \rho = \ln \left[\frac{E_0}{J_{c0}} \frac{U_0(T, B)}{kT} \right] \pm \ln \left[\sum_s f_s \exp \left[\mp \frac{U_{0s}(T, B)}{kT} \right] + \sum_n f_n (\alpha T)^{\pm 1} \right]. \quad (12)$$

The s and n indices represent superconducting and normal-metal phases, respectively, and α represents the relative scaling between the flux-creep and normal-state resistivities, i.e.,

$$\alpha \propto \left[\frac{kJ_{c0}}{E_0 U_0(T, B)} \right] \rho_{\text{onset}}. \quad (13)$$

In a percolative model, with parallel conduction channels dominating the resistive behavior, Eq. (13) shows the factor α approaches zero as J_c extrapolates to zero near the edge of the 90-K plateau. It follows that the normal-metal term cannot be ignored in the determination of $U_0(T, B)$ from the Arrhenius plots. Otherwise, the pinning energies obtained from the analysis would be in error. Equation (12) was used to fit the resistive transitions of a film grown by the BaF₂ process¹² (Fig. 5 inset) at various oxygen deficiencies δ , assuming a parallel combination of one superconducting phase with one normal-metal conduction channel. (Note that the normal-metal term could be ascribed to the collection of lower T_c , oxygen-deficient phases, which are forced normal in the temperature range of the resistive transitions). The ratio of the normal-state resistivity to the flux-creep resistivity

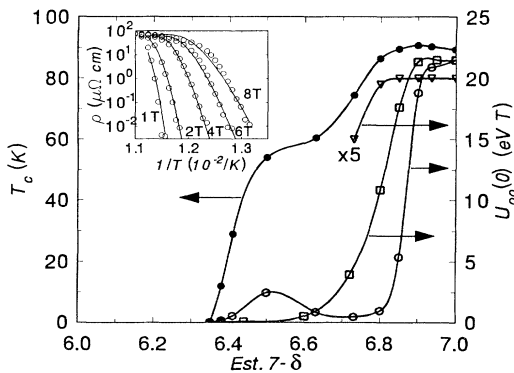


FIG. 5. Pinning energy $U_{00}(\delta) = U_0(\delta, T=0, B=1T)$ (open symbols) and $T_c(\delta)$ (solid circles) as a function of oxygen content $7 - \delta$ for a film prepared by the BaF₂ process. The open circles represent $U_{00}(\delta)$ as determined from fitting Eq. (12) to the Arrhenius curves at various oxygen deficiencies. The inset depicts an actual fit at $\delta=0$. The open squares (triangles) are $U_{00} \propto B^*$ for $H \parallel c$ ($H \parallel ab$) as defined by Eq. (14). The values of $U_{00}(\delta)$ for $H \parallel ab$ are scaled by a factor of $\frac{1}{5}$ for clarity.

at full oxygenation was assumed to be on the order of $\alpha \approx 10-100$, and was allowed to decrease with increasing oxygen deficiency according to Eq. (13). This analysis yields a plateau in the pinning energy U_0 (Fig. 5) as a function of δ near full oxygenation, even though J_c decreases in this region. In addition, a curious peak in U_0 was obtained on the 60-K plateau, possibly reflecting enhanced superconducting properties in the long-range-ordered Ortho-II phase near $\delta=0.5$. This peak also coincided with an increase in the critical current density J_c observed in this same film. Therefore, uncertainties still remain regarding the behavior of J_c and U_0 in the region of the 60-K plateau. Interestingly, the width of the plateau in U_0 vs δ varies depending upon the method used to determine U_0 (Fig. 5). Hence, it is plausible that the resistive transition model above is oversimplified in assuming the presence of only two distinct phases. Thus, unlike the case of fully oxygenated YBa₂Cu₃O₇, these plots do not appear to be a reliable means of determining the subtle behavior of $U_0(T, B)$ in oxygen-deficient YBa₂Cu₃O_{7- δ} .

The most reliable method for determining the pinning energy is an analysis of the magnetic-field dependencies of the critical current densities. This technique is unique in that knowledge of the bridge cross section is *not* required. Hettinger *et al.*³⁷ showed that the field dependence of $J_c/J_c(H=0)$ [see Fig. 3(b)] could be described by the single parameter specifying the field at which the pinning force density extrapolates linearly to zero (Fig. 6),

$$B^* = \frac{U_0 B / kT}{\ln(E_0 / 2E_c)}. \quad (14)$$

This analysis assumes that $U_0 \propto 1/B$ as experimentally observed^{33,37} and that the denominator is roughly constant. The apparent degradation seen in $J_c(\delta, H \parallel c)$ for $\delta \geq 0.15$, as well as in $J_c(\delta, H \parallel ab)$ for $\delta \geq 0.20$, is clearly attributed to a decrease in U_0 (Fig. 5). This probably leads to the progressive suppression of the $J_c(\delta, T)$ curves observed at higher temperatures [Fig. 3(a)]. The normalized flux-pinning force density at various oxygen contents both on and off the 90-K plateau are depicted in Fig. 6. Off the 90-K plateau, decreases in the relative strength of the B dependence in U_0 , similar to that found in polycrystalline films,³⁸ e.g., $U_0 \propto 1/B^{0.15}$, may occur as a result of the films developing “granularlike” critical currents for large oxygen deficiencies.

E. Constraints imposed on electronic models

If the phase-separation scenario does not apply, the initial decreases of $J_c(\delta \leq 0.15)$ could only be due to decreases in J_{c0} , since the flux-creep pinning energy U_0 is constant in this regime. Recall that J_{c0} is defined as the critical current density in the absence of flux creep and is often assumed to be proportional to the depairing critical current density. As a result, this assumption leads to the proportionality $J_{c0} \propto H_c^2 \xi_{ab}$.³⁹ Moreover, others generally argue³⁹⁻⁴² that U_0 should scale as $H_c^2 \xi^3 / 8\pi$ in a point-pinning model, where H_c is the thermodynamic

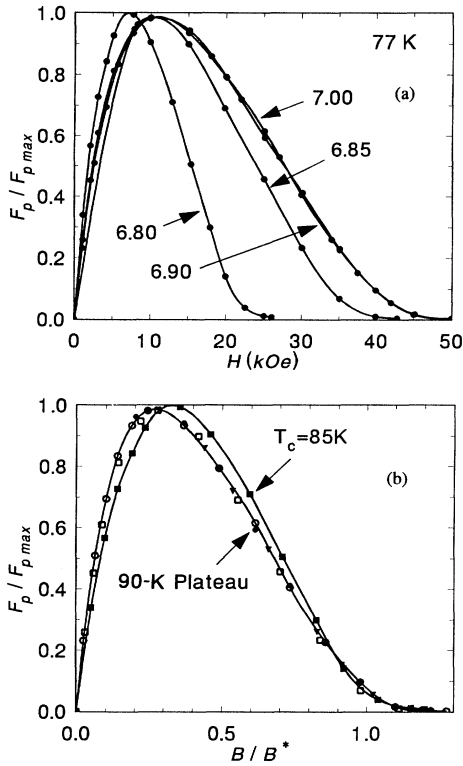


FIG. 6. Normalized pinning force density F_p taken at 77 K as a function of (a) B and (b) B/B^* as described in the text, both on and off the 90-K plateau. The universal F_p curve observed on the 90-K plateau suggests the field dependence of the pinning energy given by $U_0 \propto 1/B$ is fixed across the plateau. However, off the plateau, the relative B dependence may change, as in the polycrystalline films, (Ref. 38) leading to the observed shift in $F_{p,max}$.

critical field and ξ is the superconducting coherence length. In the highly anisotropic cuprates,⁴³ one has $\xi^3 \approx \xi_{ab}^2 \xi_c$ so that the constraint imposed by a constant U_0 becomes

$$H_c^2 \propto \frac{1}{\xi_{ab}^2 \xi_c}. \quad (15)$$

From magnetization studies, Ossandon *et al.*³² concluded that the thermodynamic critical field H_c rapidly decreases with increasing oxygen deficiency. However, if the phase-separation scenario applies, these apparent decreases in H_c could be due to a decreasing volume fraction of the 90-K phase with increasing δ . Equation (15) implies a significant increase in the coherence length ξ with increasing oxygen deficiency δ , which should be reflected as a decrease in the upper critical field, since $H_{c2} = \phi_0 / 2\pi\xi^2$. Unfortunately, conclusive systematics of H_{c2} vs δ do not yet exist. A fluctuation analysis⁴⁴ indicates the existence of an H_{c2} plateau while a Hao-Clem⁴⁵ analysis of magnetic measurements³² shows a steadily decreasing $H_{c2}(\delta)$. Thus, further information of the dependence of H_{c2} with δ would be very useful.

F. "Peaked" $T_c(\delta)$ behavior

Until now, we have not addressed the "peaked" $T_c(\delta)$ behavior (i.e., a maximum in T_c at $\delta \neq 0$), which is most apparent in epitaxial films initially grown under low-oxygen partial pressures.^{19,46} This maximum in T_c is demonstrated midway on the 90-K plateaus in T_c vs δ depicted in Figs. 2 and 5. Feenstra⁴⁷ has shown that these T_c peaks occur with systematic values of oxygen deficiency δ depending on the initial growth conditions. This implies that the location of these peaks on the 90-K plateau occur as a consequence of the level of cation "doping" introduced by the growth process. However, other mechanisms could be argued, including morphology differences or simply strains between the different phases, which are well established to have different c -lattice parameters. The latter argument appears possible since no significant splitting was observed in any of the x-ray-diffraction peaks for the films studied. However, keep in mind that one generally speaks in terms of large doping levels for the high- T_c superconductors, i.e., involving tens of percent of the unit cells, which probably alter the phonon properties as well as the electronic properties. McMillan previously showed that the coupling constant is affected by the phonon frequency spectrum.³⁶ Thus, in the framework of an electron-phonon pairing mechanism,³⁶ a more intuitive argument for these $T_c(\delta)$ peaks could simply be stated as the "optimization" of the coupling constant $\lambda = VN(E_F)$. In the coupling constant, V represents the matrix element of the electron-phonon interaction, while $N(E_F)$ is the electronic density of states at the Fermi energy E_F . Since knowledge of the phonon properties and band structure are limited, no definite conclusions on the behavior of λ as a function of doping can be drawn at the present. However, Fig. 7 illustrates the Hall coefficients for two sets of films, grown from identical precursor batches, by the BaF₂ process,¹²

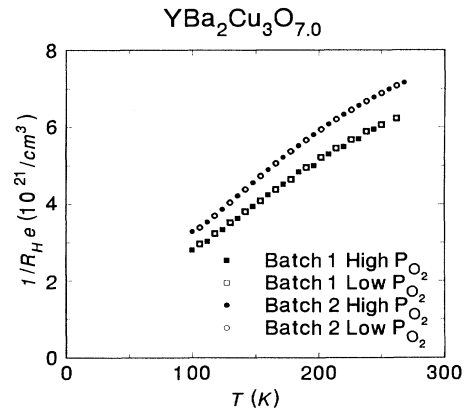


FIG. 7. Inverse Hall coefficients taken on two sets of films with identical precursors but postannealed under different conditions. The data suggest that growth conditions do not influence the overall carrier density. The slight differences between film batches may be attributed to small compositional differences in constituents or simply to errors in determining film thicknesses.

and postannealed under different conditions. The data show that the apparent carrier densities do not depend upon the initial growth conditions. The differences between films of different precursors could stem either from slight compositional differences of simply from uncertainties in the film thickness. Overall, this result implies that the processing conditions have little or no effect on the electronic structure in the fully oxygenated state. Finally, recent evidence by others suggests that lattice instabilities, and not electronic mechanisms, are indeed responsible for the limiting transition temperature of ~ 90 K observed in $\text{YBa}_2\text{Cu}_3\text{O}_{7-\delta}$.⁴⁸

V. SUMMARY

The effects of oxygen deficiency on the resistivity, Hall coefficient, and critical current density were measured on a series of twinned, epitaxial $\text{YBa}_2\text{Cu}_3\text{O}_{7-\delta}$ thin films. The inverse Hall coefficients have linear temperature dependencies, as predicted by the Luttinger liquid theory,²³ and the implied carrier densities steadily diminish with increasing oxygen deficiency δ . Moreover, the relative insensitivity of the Hall angle to oxygen deficiency suggests that only one of the four predicted electronic bands at the Fermi surface²² dominates the normal-state properties with fields $H \parallel c$. Critical currents

extrapolate to zero as the oxygen content nears the edge of the 90-K plateau, suggestive of phase separation in which only the fully oxygenated phase has the high critical current density. On the 90-K plateau, no changes are seen in the pinning energies determined from the field dependence of J_c , in general agreement with the magnetic flux-creep studies of Ossandon *et al.*³⁹ However, electronic origins cannot be ruled out at present, since the pinning energies also depend on the coherence length ξ . Moreover, information regarding H_{c2} as a function of δ is inconclusive.^{32,44} Overall, the phase-separation scenario appears to be a viable candidate for explaining many experimental observations.

ACKNOWLEDGMENTS

The authors acknowledge the beneficial, and often diverse, suggestions offered by R. C. Dynes, W. E. Pickett, S. A. Wolf, G. Deutscher, R. Beyers, J. Yu, J. D. Mahan, R. S. Markiewicz, and J. Clayhold. The authors are grateful to B. C. Chakoumakos for carefully reading this manuscript. Research sponsored by the Division of Materials Sciences, U. S. Department of Energy under Contract No. DE-AC05-84OR21400, with Martin-Marietta Energy Systems, Inc.

*Current address: Sandia National Laboratories, Division 1154, P.O. Box 5800, Albuquerque, NM 87185.

¹R. J. Cava, B. Batlogg, C. H. Chen, E. A. Rietman, S. M. Zahurak, and D. Werder, *Phys. Rev. B* **36**, 5719 (1987).

²M. Däumling, L. E. Levine, and T. M. Shaw, in *Advances in Cryogenic Engineering Materials*, edited by F. R. Fickett and R. P. Reed (Plenum, New York, 1992), Vol. 38, p. 949.

³C. Namgung, J. T. S. Irvine, and A. R. West, *Physica C* **168**, 346 (1990).

⁴V. Z. Kresin, S. A. Wolf, and G. Deutscher, *Physica C* **191**, 9 (1992).

⁵R. McCormack, D. de Fontaine, and G. Ceder, *Phys. Rev. B* **45**, 12 976 (1992).

⁶B. W. Veal and A. P. Paulikas, *Physica C* **184**, 321 (1991).

⁷M. S. Osofsky, J. L. Cohn, E. F. Skelton, M. M. Miller, R. J. Soulen, Jr., S. A. Wolf, and T. A. Vanderah, *Phys. Rev. B* **45**, 4916 (1992).

⁸J. L. Vargas and D. C. Larbalestier, *Appl. Phys. Lett.* **60**, 1741 (1992).

⁹R. Beyers, B. T. Ahn, G. Gorman, V. Y. Lee, S. S. P. Parkin, M. L. Ramirez, K. P. Roche, J. E. Vazquez, T. M. Gür, and R. A. Huggins, *Nature* **340**, 619 (1989).

¹⁰D. J. Werder, C. H. Chen, R. J. Cava, and B. Batlogg, *Phys. Rev. B* **38**, 5130 (1988).

¹¹T. Zeiske, R. Sonntag, D. Hohlwein, N. H. Andersen, and T. Wolf, *Nature* **353**, 542 (1991).

¹²M. P. Siegal, J. M. Phillips, A. F. Hebard, R. B. van Dover, R. C. Farrow, T. H. Tiefel, and J. H. Marshall, *J. Appl. Phys.* **70**, 4982 (1991).

¹³Shen Zhu, Douglas H. Lowndes, X.-Y. Zheng, David P. Norton, and R. J. Warmack, in *Interface Dynamics and Growth*, edited by K. S. Liang, M. P. Anderson, R. F. Bruinsma, and G. Scoles, MRS Symposia Proceedings No. 237 (Materials Research Society, Pittsburgh, 1991), p. 541.

¹⁴R. Feenstra, T. B. Lindemer, J. D. Budai, and M. D. Gallo-way, *J. Appl. Phys.* **69**, 6569 (1991).

¹⁵C. M. Hurd, *The Hall Effect in Metals and Alloys* (Plenum, New York, 1972).

¹⁶R. Feenstra has shown this to be a universal result in thin films (unpublished).

¹⁷R. J. Cava, A. W. Hewat, E. A. Hewat, B. Batlogg, M. Marezio, K. M. Rabe, J. J. Krajewski, W. F. Peck, Jr., and L. W. Rupp, Jr., *Physica C* **165**, 419 (1990).

¹⁸J. D. Jorgensen, B. W. Veal, A. P. Paulikas, L. J. Nowicki, G. W. Crabtree, H. Claus, and W. K. Kwok, *Phys. Rev. B* **41**, 1863 (1990).

¹⁹R. Feenstra, D. K. Christen, C. E. Klabunde, and J. D. Budai, *Phys. Rev. B* **45**, 7555 (1992).

²⁰B. W. Veal, A. P. Paulikas, Hoydoo You, Hao Shi, Y. Fang, and J. W. Downey, *Phys. Rev. B* **42**, 6305 (1990).

²¹J. M. Ziman, *Principles of the Theory of Solids*, 2nd ed. (Cambridge, New York, 1972).

²²H. Krakauer, W. E. Pickett, and R. E. Cohen, *J. Supercond.* **1**, 111 (1988).

²³P. W. Anderson, *Phys. Rev. Lett.* **67**, 2092 (1991).

²⁴R. S. Markiewicz, *Physica C* **177**, 445 (1991).

²⁵C. C. Tsuei, C. C. Chi, D. M. News, P. C. Pattnaik, and M. Däumling (unpublished).

²⁶O. K. Andersen, A. I. Liechtenstein, O. Rodriguez, I. I. Mazin, O. Jepsen, V. P. Antropov, O. Gunnarsson, and S. Gopalan, *Physica C* **185-189**, 147 (1991).

²⁷W. E. Pickett, *Rev. Mod. Phys.* **61**, 433 (1989).

²⁸J. Yu (private communication).

²⁹P. B. Allen, W. E. Pickett, and H. Krakauer, *Phys. Rev. B* **37**, 7482 (1988).

³⁰N. P. Ong, *Phys. Rev. B* **43**, 193 (1991).

³¹A. T. Fiory and G. S. Grader, *Phys. Rev. B* **38**, 9198 (1988).

³²J. G. Ossandon, J. R. Thompson, D. K. Christen, B. C. Sales,

- H. R. Kerchner, J. O. Thomson, Y. R. Sun, K. W. Lay, and J. E. Tkaczyk, *Phys. Rev. B* **45**, 12 534 (1992).
- ³³S. Zhu, D. K. Christen, C. E. Klabunde, J. R. Thompson, E. C. Jones, R. Feenstra, D. H. Lowndes, and D. P. Norton, *Phys. Rev. B* **46**, 5576 (1992).
- ³⁴Guy Deutscher, in *Percolation, Localization and Superconductivity*, edited by Allen M. Goldman and Stuart A. Wolf (Plenum, New York, 1984), p. 95.
- ³⁵R. Wördenweber, *Phys. Rev. B* **46**, 3076 (1992).
- ³⁶M. Tinkham, *Introduction to Superconductivity* (McGraw-Hill, New York, 1975).
- ³⁷J. D. Hettinger, A. G. Swanson, W. J. Skocpol, J. S. Brooks, J. M. Graybeal, P. M. Mankiewich, R. E. Howard, B. L. Straughn, and E. G. Burkhardt, *Phys. Rev. Lett.* **62**, 2044 (1989).
- ³⁸E. C. Jones, D. K. Christen, C. E. Klabunde, J. R. Thompson, D. P. Norton, R. Feenstra, D. H. Lowndes, and J. D. Budai, *Appl. Phys. Lett.* **59**, 3183 (1991).
- ³⁹J. G. Ossandon, J. R. Thompson, D. K. Christen, B. C. Sales, Y. Sun, and K. W. Lay, *Phys. Rev. B* **46**, 3050 (1992).
- ⁴⁰P. W. Anderson, *Phys. Rev. Lett.* **9**, 309 (1962).
- ⁴¹Y. B. Kim, *Rev. Mod. Phys.* **36**, 39 (1964).
- ⁴²M. V. Feigel'man, V. B. Geshkenbein, and A. I. Larkin, *Physica C* **167**, 177 (1990).
- ⁴³Y. Yeshurun and A. P. Malozemoff, *Phys. Rev. Lett.* **60**, 2202 (1988).
- ⁴⁴E. C. Jones, D. K. Christen, J. R. Thompson, J. G. Ossandon, R. Feenstra, J. M. Phillips, and M. P. Siegal (unpublished).
- ⁴⁵Z. Hao, J. Clem, M. McElfresh, L. Civale, A. Malozemoff, and F. Holtzberg, *Phys. Rev. B* **43**, 2844 (1991).
- ⁴⁶V. Matijasevic, P. Rosenthal, K. Shinohara, A. F. Marshall, R. H. Hammond, and M. R. Beasley, *J. Mater. Res.* **6**, 682 (1991).
- ⁴⁷R. Feenstra (unpublished).
- ⁴⁸M. Lang, R. Kürsch, A. Grauel, C. Geibel, F. Steglich, H. Rietschel, T. Wolf, Y. Hidaka, K. Kumagai, Y. Maeno, and T. Fujita, *Phys. Rev. Lett.* **69**, 482 (1992).
- ⁴⁹K. K. Likharev, *Rev. Mod. Phys.* **51**, 115 (1979).